What determines the maximum sea ice extent in the Sea of Okhotsk? Importance of ocean thermal condition from the Pacific

Takuya Nakanowatari,[1] Kay I. Ohshima,[1] and Sachiko Nagai[1,2]

Received 20 December 2009; revised 13 August 2010; accepted 22 September 2010; published 15 December 2010.

[1] Previous studies suggested that the interannual variability of the maximum sea ice extent (MSIE) in the Sea of Okhotsk is not explained only by atmospheric conditions. In this study, we examined the effect of the ocean thermal condition on the determination of the MSIE based on observational data. We found that the MSIE is highly correlated with the sea surface temperature (SST) and ocean temperature around the East Kamchatska Current (EKC) in the Pacific in late autumn (November–December). The significant relationship between the MSIE and the SST cannot be fully explained by prevailing atmospheric variabilities. Considering that the inflow of EKC water to the Okhotsk Sea is strengthened in winter, advection of anomalous ocean temperature likely influences the MSIE. A multiple regression model constructed as a function of SST in the EKC and the air temperature at 850 hPa over the upwind region of the Okhotsk Sea in late autumn, which is another determinant factor for the MSIE, significantly improves the prediction skill for the MSIE: 70% of the variance of MSIE can be predicted at the stage of 2 to 3 months before the MSIE season. The SST in the EKC and the upwind air temperature are likely to control the sea ice extent in the northeastern and center to southern parts of the Okhotsk Sea, respectively.

Citation: Nakanowatari, T., K. I. Ohshima, and S. Nagai (2010), What determines the maximum sea ice extent in the Sea of Okhotsk? Importance of ocean thermal condition from the Pacific, *J. Geophys. Res.*, *115*, C12031, doi:10.1029/2009JC006070.

1. Introduction

[2] The Sea of Okhotsk is a marginal sea located on the northwest rim of the Pacific Ocean and the southernmost sea with sizable seasonal ice cover in the Northern Hemisphere. In winter, sea ice formation begins from the northwestern shelf in November. The sea ice extent becomes maximum in late February to early March, covering 50%–90% of the sea, and most of the ice disappears by May. The sea ice cover acts as insulation to obstruct the heat flux between the ocean and atmosphere [*Inoue et al.*, 2003]. *Honda et al.* [1999] suggested that sea ice anomalies in the Sea of Okhotsk cause anomalous heat fluxes at the ocean surface, and then influence the global-scale atmospheric circulation through the propagation of stationary Rossby waves. Recently, it has been reported that the yearly sea ice extent in the Sea of Okhotsk has revealed a decreasing trend (−25%/30 yr), although the year-to-year variation is dominant [*Parkinson and Cavalieri*, 2008]. It is likely that the sea ice extent in the Sea of Okhotsk is sensitive to global warming.

[3] The cause of variability of sea ice extent in the Sea of Okhotsk has been investigated mostly in terms of the relation to atmospheric conditions [*Cavalieri and Parkinson*, 1987; *Parkinson*, 1990; *Tachibana et al.*, 1996; *Yamazaki*, 2000; *Ogi and Tachibana*, 2006; *Sasaki et al.*, 2007]. According to *Kimura and Wakatsuchi* [1999], the maximum sea ice extent (MSIE) is well explained by ice drift due to geostrophic wind speed from 1987 to 1997, but not from 1978 to 1986, in which the MSIE is relatively large. *Ohshima et al.* [2006] showed that the onset of sea ice formation is mostly determined by the local heat flux in the preceding autumn (October–November), while they suggested that the effect of the local heat flux on the sea ice extent becomes weak in the late stage of the ice covered season. These results imply that the MSIE is not explained only by atmospheric conditions.

[4] It is known that relatively warm water which originates from the East Kamchatska Current (EKC) flows into the Sea of Okhotsk through the northern Kuril Straits. Even in midwinter, the region to which this warm water arrives is not covered with sea ice in most years except for 1979, 1980, and 2001, in which almost all areas of the Sea of Okhotsk were covered with sea ice (Figure 1). Therefore, it is expected that warm water advection from the Pacific is an important factor in determining the MSIE. Recently, it was suggested that the autumn atmospheric heat condition affects the MSIE through the ocean thermal persistence in

[1] Institute of Low Temperature Science, Hokkaido University, Sapporo, Japan.
[2] Now at ITO-Ya Company, Tokyo, Japan.

0148-0227/10/2009JC006070

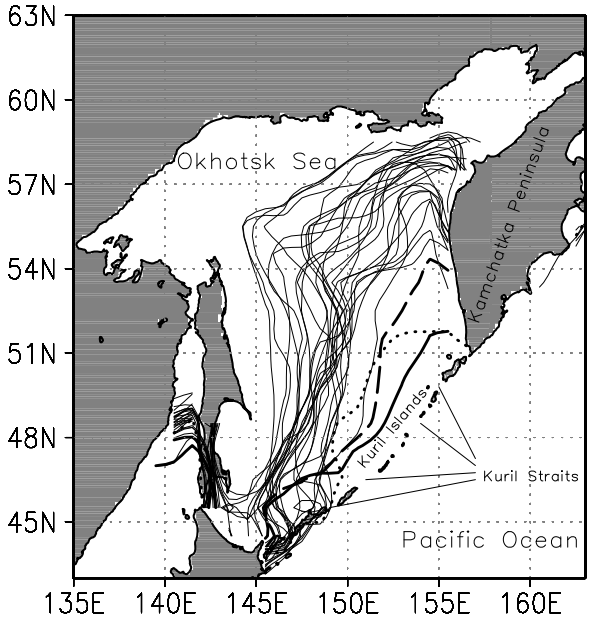

Figure 1. The mean sea ice edges (contours) in February–March from 1979 to 2006. The mean sea ice edge is defined as the boundary of 30% sea ice concentration averaged in February–March. The sea ice edges in 1979, 1980, and 2001 are shown by thick solid, long dashed, and dotted lines, respectively.

the Sea of Okhotsk [*Sasaki et al.*, 2007]. However, the variation in the ocean temperature in itself has not been examined yet.

[5] In this study, we assess the effect of oceanic thermal condition on MSIE variations by examining historical oceanographic data, recent observations conducted in the Sea of Okhotsk from 1998 to 2004 and high-resolution satellite estimates. The paper is organized in the following manner. Data and methods are described in section 2. The relationship between the MSIE and ocean thermal condition is described by analyzing the sea surface temperature (SST) data and the newly made upper ocean temperature data in section 3. In this section, we also examine the effect of atmospheric condition and ocean current field on the ocean thermal condition. In section 4, we propose an improved prediction scheme for the MSIE, based on our new analysis. Section 5 closes the paper with summary and discussion.

2. Data and Methods

[6] Sea ice concentration data for the Sea of Okhotsk were derived from the Hadley Centre sea Ice and Sea Surface Temperature data set version 1 (HadISST) from 1979 to 2006 [*Rayner et al.*, 2003]. The sea ice area was calculated by averaging the area weighted by sea ice concentration in the entire Sea of Okhotsk; the MSIE is defined by the sea ice area averaged from February to March. The derived MSIE data are almost identical to those obtained from other data sources by the Japan Meteorological Agency (JMA) and by *Kimura and Wakatsuchi* [1999]. Use of the sea ice extent averaged from mid-February to mid-March as MSIE does not change the results.

[7] As sea surface temperature (SST) data, we mainly used the monthly mean SST data derived from the HadISST [*Rayner et al.*, 2003] on a 1° × 1° latitude-longitude grid from 1979 to 2006. The SST data in grid boxes where sea ice concentration is larger than 5% were not used in this study. Although the HadISST data set provides reliable SST data when in situ observations and/or satellite estimation are available, there is concern that this data set sometimes provides data even for grid boxes with no observations, through some interpolation procedure. To validate the result from the HadISST, we used the monthly mean SST data from the International Comprehensive Ocean-Atmosphere Data Set version 2.4 (ICOADS) 2° × 2° products [*Worley et al.*, 2005], which are based only on in situ observations, allowing no-data grid boxes. We also used the Advanced Very High Resolution Radiometer (AVHRR) infrared satellite SST data with 0.25° resolution from 1982 to 2006 [*Reynolds et al.*, 2007]. Information of the AVHRR data is also included in the HadISST from 1982, but the spatial resolution of this SST data set is higher. The annual cycle was excluded from the monthly mean data by subtracting climatological monthly means from individual months.

[8] For ocean temperature, we prepared a new data set based on in situ oceanographic observations from the World Ocean Database 2005 (WOD05) [*Boyer et al.*, 2006] with additional data archived by the Japan Oceanographic Data Center and those obtained by the Japan-Russia-U.S. international joint study of the Sea of Okhotsk, including 20 profiling float data from 2000 to 2004. The monthly temperature climatologies were calculated at standard levels for each 1° latitude/longitude grid box by a method similar to that of *Levitus and Boyer* [1994]. Since water mass properties in the Sea of Okhotsk are distinctly different from those in the northwestern North Pacific, we produced their gridded data set separately. For constructing the gridded data set, we used weighted averaging with a Gaussian window. We chose 200 km as the half-width of the window and 100 km as the e-folding scale. If the number of observations within the window was less than 5, that grid box was regarded as a no-data box. Since the decrease rate of ocean temperature is large in November–December, the difference between the beginning and end of the month should be taken into account. Thus, the monthly climatology is interpolated to 5 day intervals using the first four sinusoidal components (annual, semiannual, 4 month, and 3 month components). The anomaly was calculated as raw temperature value minus the climatological mean value on the corresponding date.

[9] For seasonal and interannual variation in the ocean surface current, the merged products of monthly mean sea surface height anomaly (SSHA) from Topex/Poseidon, Jason-1, and European Research Satellite altimeter observations from 1993 to 2006 were used. The sea level anomalies were produced by the French Archiving, Validation, and Interpolation of Satellite Oceanographic Data (AVISO) project using the mapping method of *Ducet et al.* [2000]. The monthly mean SSHA was calculated from the annual mean SSH data from 1993 to 1999. Therefore, the monthly mean SSHA includes the seasonal variation as well as the interannual variation. To remove the SSHA related to mesoscale eddies, we used SSHA data which are linearly interpolated onto 1° latitude/longitude grid. We also used

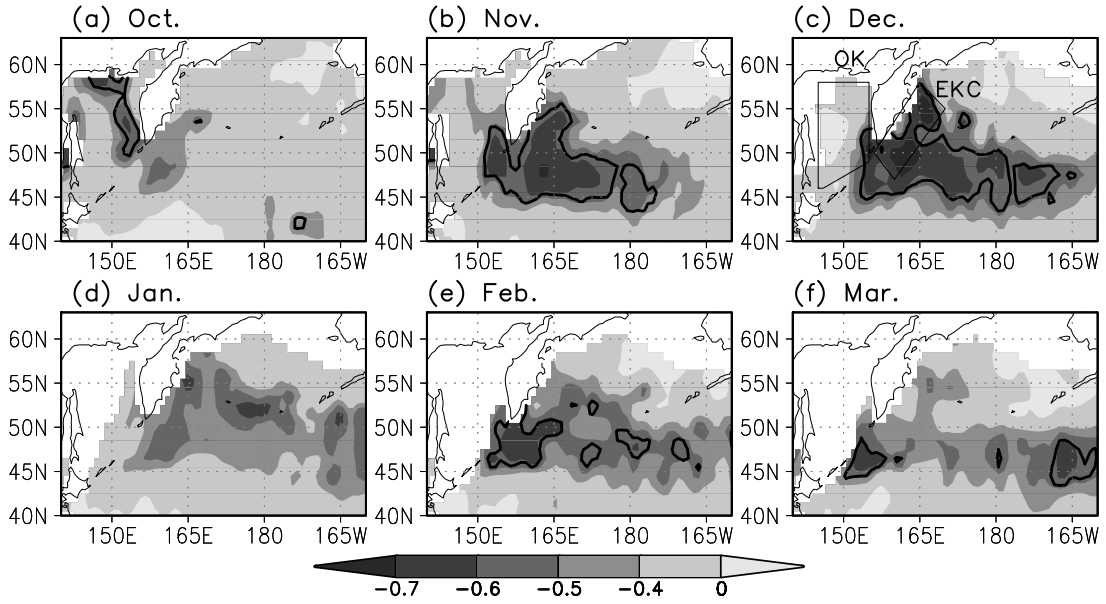

Figure 2. (a–f) Lag correlation maps between the MSIE and SST in the preceding October–March derived from HadISST. Thick contours indicate areas where the correlation exceeds the 99% confidence level. The significance of correlations is estimated by a Monte Carlo simulation, using a phase randomization technique generating 1000 surrogate time series [*Kaplan and Glass*, 1995].

dynamic topography calculated from climatological ocean temperature and salinity data of our data set. The climatology of salinity was made in the same method as that of ocean temperature.

[10] The meteorological data are derived from the monthly mean National Centers for Environmental Prediction/Department of Energy (NCEP/DOE) reanalysis data [*Kanamitsu et al.*, 2002].

3. Relationship Between the MSIE and Ocean Thermal Condition

3.1. Analysis of SST and Ocean Data Set

[11] Figure 2 shows the lag correlation map between the MSIE and the monthly SST anomalies from the preceding October to March. We found that the MSIE has the highest negative correlation with the SSTs in the northwestern part of the North Pacific in the preceding November–December (Figures 2b and 2c). Particularly high correlation (absolute value larger than 0.7) is found in and around the East Kamchatska Current (EKC). The lag correlation analysis between the MSIE and SSTs in the EKC region (rectangular box shown in Figure 2c) shows that the negative correlation between them becomes highest ($r = -0.72$) when the SSTs lead the MSIE by 2–3 months (Figure 3). Similar results are also found in the lagged correlation between the MSIE and the SST anomalies derived from the ICOADS SST data, although the absolute value of the correlation is somewhat smaller than that of HadISST (Figure 3). The correlation between the ICOADS SST in the preceding November–December and the MSIE is −0.58, which is significant at the 95% confidence level.

[12] Next, we examine the ocean data set which we newly made, by comparing with the MSIE. Since the ocean data are too limited to show the spatial features of the correlation, we treat the averaged data in the EKC region (rectangular box in Figure 2c). The correlations between the MSIE and the temperature of the upper 30 m are significant at the 95% confidence level (Figure 4a). The correlation abruptly becomes small (insignificant) at depths deeper than 50 m. According to the vertical profile of the climatological potential density averaged in the EKC region in November–December (Figure 4b), the mixed layer depth is found to be ~50 m. This result suggests that the ocean temperature anomaly in the mixed layer is related to the MSIE variation. Figure 5 compares the time series of the MSIE anomalies with those of the SSTs and the ocean temperature anomalies at 20 m depth in the EKC region in the preceding November–December, demonstrating that both the SSTs and ocean temperature anomalies show good correspondence with the

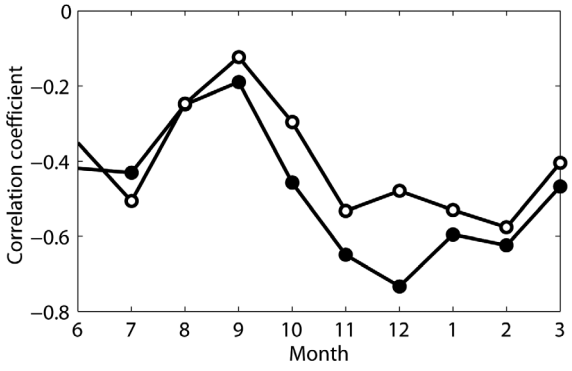

Figure 3. Lagged correlation coefficients between the MSIE and the monthly SST anomaly of HadISST (solid circles) and ICOADS (open circles) averaged over the EKC region. The area of averaging is shown as a rectangular box in Figure 2c.

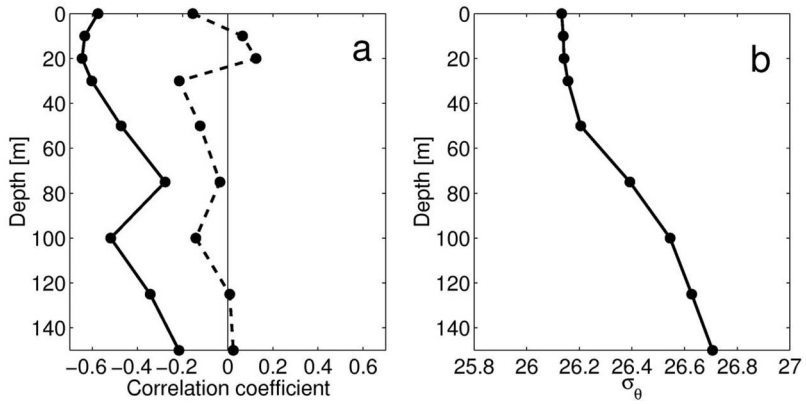

Figure 4. (a) Correlation coefficients between the MSIE and upper ocean temperature from the surface to 150 m depth in the preceding November–December averaged over the EKC region (solid line) and the Sea of Okhotsk (dashed line). (b) The climatology of the potential density from the surface to 150 m depth in November–December averaged over the EKC region. The areas of averaging are shown as rectangular boxes in Figure 2c.

MSIE anomalies all through the analyzed period. For example, the minimum value of the ocean temperature anomaly in November–December 2000 is consistent with the largest MSIE anomaly in 2001.

[13] On the other hand, the correlation between the MSIE and SST within the Sea of Okhotsk is much smaller than that for the EKC region in the preceding November–December (Figures 2b and 2c), except in the region around the northern part of the Kuril Straits. The ocean temperature data set which was newly made also shows a consistent result: the correlation between the MSIE and the ocean temperature averaged in the central to southern parts of the Okhotsk Sea (area indicated in Figure 2c) in November–December is less than 0.2 for all depths (Figure 4a).

[14] Even in January, just before the MSIE month (Figure 2d), significant correlation between the MSIE and SST cannot be found in the Sea of Okhotsk. This might be due to rough spatial resolution of the HadISST under the very limited in situ observation and unreliable satellite data by the existence of sea ice. Thus, we analyzed the AVHRR SST data set, which has higher spatial resolution and is expected to be more reliable near sea ice edge region, although the data are only available from 1982. Figure 6 shows the correlation map of the monthly mean AVHRR SST with the MSIE. In the preceding November, significant negative correlation (absolute value is larger than 0.6) is found in the EKC region as in the case of the HadISST. On the other hand, significant correlation is not found within the Sea of Okhotsk at the stage of the November. In the preceding December and January, however, significant negative correlation is found in the eastern part of the Okhotsk Sea, particularly along the west coast of the East Kamchatska Peninsula.

3.2. Effect of Prevailing Atmospheric Variability

[15] One might think that prevailing atmospheric variabilities affects both the MSIE and the SST in the EKC region in late autumn and that the high correlation between the MSIE and SST is apparent one. This concern arises from the significant negative correlation between the MSIE and the SST over the western subarctic gyre all through the preceding November–March (Figures 2b–2f). These significant negative correlations may be partly related to the local atmospheric condition over the Okhotsk Sea in late autumn [*Sasaki et al.*, 2007] and winter [e.g., *Kimura and Wakatsuchi*, 1999] and the dominant atmospheric modes in the northern hemisphere of the Aleutian low strength [e.g., *Tachibana et al.*, 1996], the North Atlantic Oscillation (NAO) [*Deser et al.*, 2000], and the Arctic Oscillation (AO) [*Ogi and Tachibana*, 2006]. Therefore, we checked the possibility that these atmospheric variabilities determine both the SST in the EKC region and the MSIE.

[16] First, we evaluated the contributions of the autumn and wintertime atmospheric conditions over the Sea of Okhotsk. For the autumn atmospheric condition, we adopt the air temperature at 850 hPa (T850) in October–November in the upwind region of the Sea of Okhotsk (52.5°N, 135°E), following *Sasaki et al.* [2007]. They showed that the T850 is

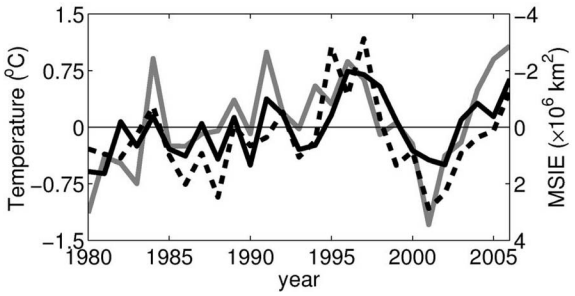

Figure 5. Time series of SST anomalies (solid black line); ocean temperature anomalies at 20 m depth (broken line), averaged in the EKC region (the rectangular box in Figure 2c) in November–December; and the MSIE anomalies (gray line). For calculation of the ocean temperature in 1994, 1997, and 2001, the EKC region is extended offshore twice because the in situ ocean data were extremely limited within the box. The time series of SST and ocean temperature anomalies are shifted by 1 year (the preceding year). The scale of the MSIE anomalies is indicated on the right axis and inverted.

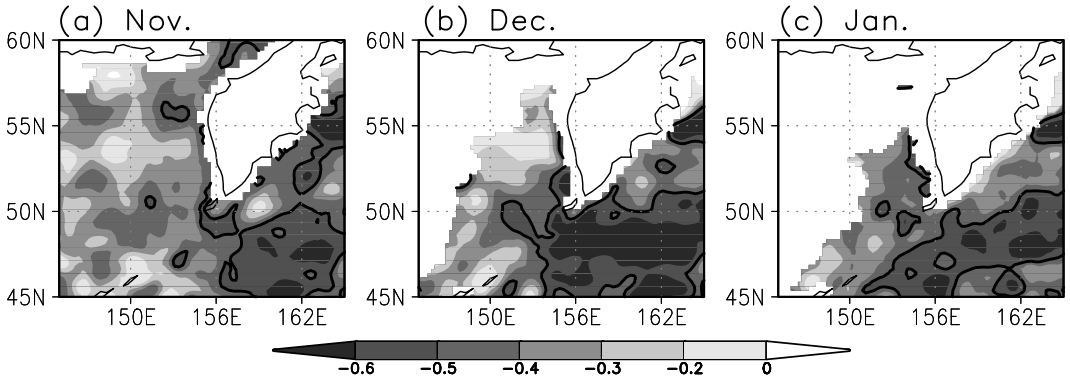

Figure 6. Lag correlation maps between the MSIE and SST in the preceding (a) November, (b) December, and (c) January derived from the AVHRR SST data from 1982 to 2006 in the center to eastern part of the Sea of Okhotsk and EKC region. Thick contours indicate areas where the correlation exceeds the 95% confidence level.

most highly correlated with the MSIE among various atmospheric factors in the preceding autumn. For the wintertime atmospheric condition, we use geostrophic wind rather than the air temperature, because the air temperature is significantly influenced by ocean/sea ice condition below [*Inoue et al.*, 2003]. The wintertime atmospheric index is defined by the NW-SE component of the geostrophic wind (V_g) over the Sea of Okhotsk (50°N–60°N, 145°E–165°E) in December–February, following *Kimura and Wakatsuchi* [1999].

[17] The correlation relationships among the MSIE, SST in the EKC region in the preceding November–December, T850, and V_g are summarized in Table 1. The correlation of the T850 with the MSIE is −0.71 (significant at the 95% confidence level), which is consistent with *Sasaki et al.* [2007]. This high correlation is comparable to that between the MSIE and the SST (−0.72). These two factors seem to be somewhat related with each other, but not strongly (the correlation between them is 0.46). As shown by several previous studies [e.g., *Kimura and Wakatsuchi*, 1999], V_g is positively correlated with the MSIE (r = 0.41), but the correlation is much smaller than those for the SST and T850. The correlation between the T850 (or SST) and V_g is also small.

[18] To specify the area of ice extent variability related to these factors, we calculate the correlation map of the sea ice concentration averaged in February–March with the SST in the EKC region in the preceding November–December, T850, and V_g. Figure 7a shows the correlation map of the sea ice concentration with the SST. A significant negative correlation is found in the northeastern part of the Sea of Okhotsk. On the other hand, the T850 is significantly correlated with the sea ice concentration in the central to southern part (Figure 7b), which is clearly different from that for the SST. The correlation map for the V_g is similar to that for the T850, but the absolute value of the correlation is relatively small (Figure 7c).

[19] To examine whether a high correlation between the SST and MSIE is a result of the prevailing atmospheric variabilities or not, we make a following multiple regression analysis. First, the multiple regression coefficients of the MSIE and SST onto the T850 and V_g are calculated. Then the residual time series of the MSIE and SST that excludes the T850 and V_g components are calculated and defined as rMSIE and rSST, as follows:

$$rMSIE = MSIE - \left(\alpha_1 T850 + \alpha_2 V_g\right), \quad (1)$$

$$rSST = SST - \left(\beta_1 T850 + \beta_2 V_g\right), \quad (2)$$

where, $\alpha_1(\beta_1)$ and $\alpha_2(\beta_2)$ are the multiple regression coefficients of the MSIE (SST) onto the T850 and V_g. If rSST and rMSIE are significantly correlated with each other, it is concluded that the significant correlation between the MSIE and SST is not apparent one by these atmospheric variabilities.

[20] Figure 8 shows that the lag correlation map between the rMSIE and the monthly rSST anomalies. Overall, the absolute values of the correlation coefficients become smaller than the case of original time series (Figure 2), but the significant negative correlations are still found in the EKC region in the preceding November–December. On the other hand, the significant correlations over the western subarctic gyre in February–March found in Figure 2 vanish, indicating that significant correlations in these regions are strongly affected by these atmospheric conditions. The correlation between the rSST in the EKC region in the preceding November–December and the rMSIE becomes slightly smaller (−0.65) than the original time series (−0.72), but the correlation is still significant at the 99% confidence level. This result rejects that the significant correlation

Table 1. Correlations Among the MSIE, SST, T850, and V_g[a]

	MSIE	SST	T850	V_g
MSIE	–	**−0.72**	**−0.71**	0.41
SST	–	–	0.46	0.14
T850	–	–	–	0.39
V_g	–	–	–	–

[a]SST, T850, and V_g are defined by the sea surface temperature averaged over the EKC region in the preceding November–December; air temperature at 850 hPa in the preceding October–November at 52.5°N, 135°E; and the offshore component of the wintertime geostrophic wind (December–February) over the Sea of Okhotsk (50°N–60°N, 145°E–165°E), respectively. Bold numbers indicate the correlations exceeding the 95% confidence level based on the Monte Carlo simulation.

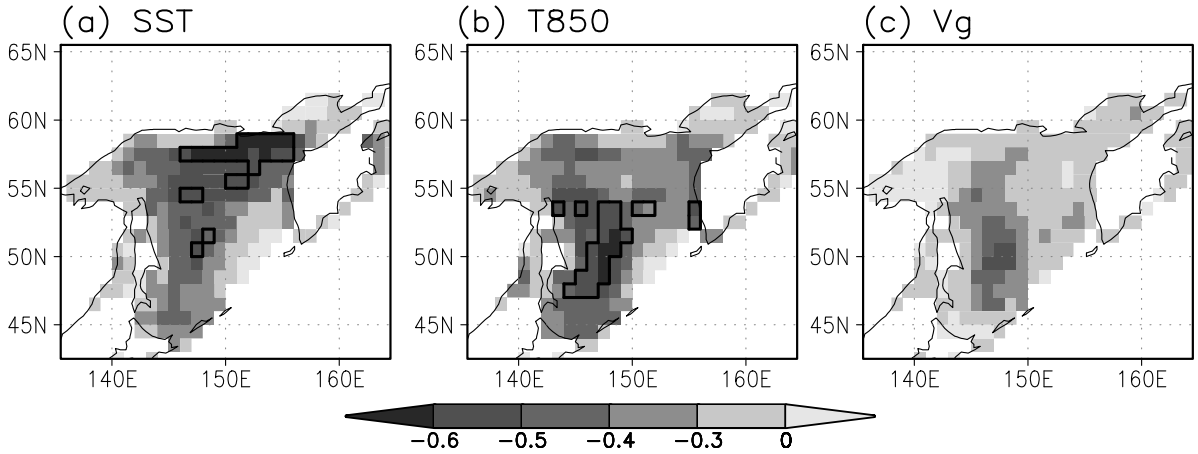

Figure 7. Correlation maps between the sea ice concentration in February–March and (a) SST averaged over the EKC region in the preceding November–December, (b) T850 at 52.5°N, 135°E in the preceding October–November, and (c) the NW-SE component of the geostrophic wind over the Sea of Okhotsk (50°N–60°N, 145°E–165°E) in December–February. Thick contours indicate areas where the correlation exceeds the 99% confidence level.

between the SST in the EKC and the MSIE is apparent one by the prevailing atmospheric variabilities.

[21] Next, we examine the effects of the dominant atmospheric modes in the northern hemisphere on the SST and MSIE. For the indexes of the NAO and AO, we used the NAO index (NAOI) and AO index (AOI) provided by the NOAA Climate Prediction Center on their web site. As the index of the strength of the Aleutian low, we used the North Pacific Index (NPI), which is a sea level pressure time series averaged over a region from 30°N–65°N, 160°E–140°W [*Trenberth and Hurrell*, 1994]. The correlation of the MSIE with the NPI, NAOI, and AOI in February–March are −0.23, −0.00, and −0.04, respectively. The correlation of the SST in the EKC with the NPI, NAOI, and AOI in November–December are 0.06, −0.35, and −0.05, respectively. The correlations of the MSIE and SST with these indexes leading by one to several months are still low and insignificant.

[22] To evaluate the effect of the annual AO shown by *Ogi and Tachibana* [2006], we also calculate the correlation between the annual mean AOI in the preceding year and the MSIE, but the correlation is low (−0.17) and insignificant. On the other hand, the correlation between them with 5 year low-pass filter is −0.41. Thus, the MSIE is partly related to

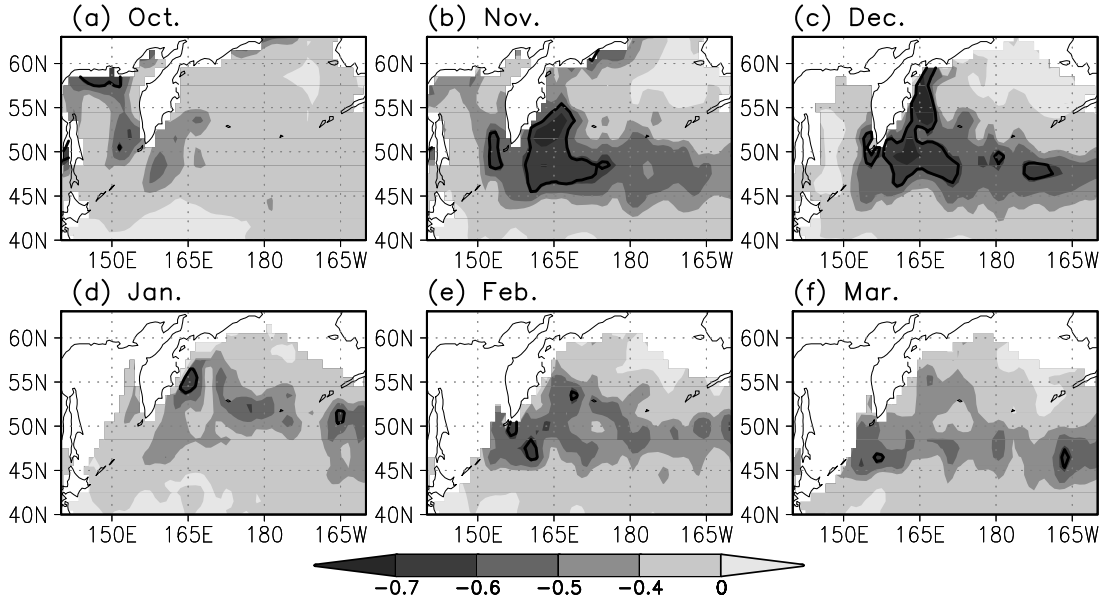

Figure 8. Same as in Figure 2 but for the correlation maps between the rSST and the rMSIE, which are the SST and MSIE from which the contributions of the T850 and V_g are excluded by the multiple regression analysis (see text for details).

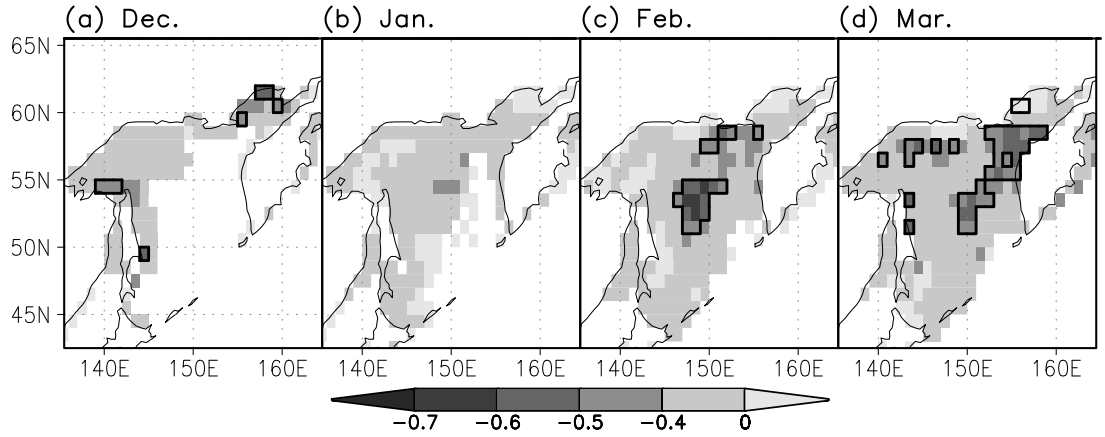

Figure 9. Correlation maps of the sea ice concentration in (a) December, (b) January, (c) February, and (d) March with the SST averaged over the EKC region in the preceding November–December. In this analysis, the contributions of the T850 and V_g are excluded from both the sea ice extent and the SST by the multiple regression analysis. Thick contours indicate areas where the correlation exceeds the 95% confidence level.

the annual AO on multiyear timescale, as shown by *Ogi and Tachibana* [2006], but the year-to-year variability cannot be fully explained by the annual AO as well as the global atmospheric modes of the NAO and the Aleutian low strength.

3.3. Ocean Current Field

[23] Since the SST variation in the EKC region leads the MSIE variation by 2–3 months (Figure 3), and the SST variation in the eastern part of the Sea of Okhotsk in January, just before the MSIE months, is significantly correlated with the MSIE variation (Figure 6c), it is expected that the MSIE variation is controlled by inflowing water from the Pacific. Figure 9 shows the lag correlation map of the sea ice concentration with the SST in the EKC region in the preceding November–December from which the contributions of T850 and V_g are excluded by the multiple regression analysis as in equations (1) and (2). The significant correlation is not found in the preceding December–January. On the other hand, the significant negative correlation is found in the northeastern part of the Okhotsk Sea in February–March as shown in Figure 7a. This result indicates a time lag of 2–3 month between the SST in the EKC and the MSIE variation.

[24] Here, we explore the surface ocean circulation, with attention paid to the EKC and its inflow to the Sea of Okhotsk. Figure 10a shows the wintertime (January–February) sea surface height anomaly (SSHA) field averaged from 1993 to 2006. High SSHA is found on both sides of the Kamchatska Peninsula, indicating that the EKC and its inflow to the Sea of Okhotsk through the northern Kuril Straits are strengthened in winter. A seasonal variation in the water exchange between the Sea of Okhotsk and Pacific is also suggested by observational data [*Ohshima et al.*, 2010]. They showed that the inflow to the Sea of Okhotsk through the northern Kuril Straits and the outflow to the Pacific through the southern straits are strengthened in winter. Numerical model simulation also supports that the water exchange is prominent in winter, and indicates that the inflow water volume through the northeastern straits reaches 10 Sv [*Katsumata and*

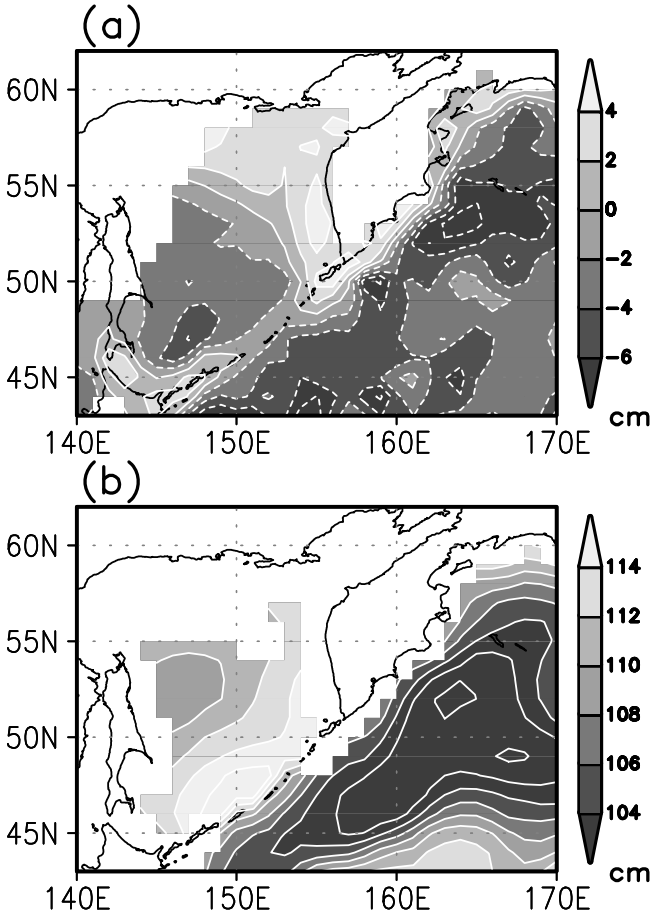

Figure 10. (a) Sea surface height anomaly field (cm) in January–February, averaged from 1993 to 2006, and (b) dynamic topography (cm) of 100 m surface relative to 1000 dbar calculated by the annual mean climatology of our data set. The contour interval is 2 cm. For calculation of surface dynamic topography in the area shallower than the reference level, extrapolation from the deeper area is made on the steric height at the bottom.

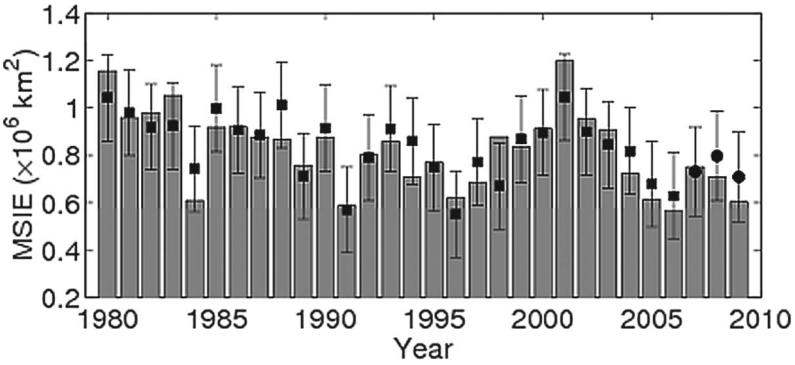

Figure 11. Time series of the predicted MSIE from scheme (3) (black squares) and observed MSIE (gray bars). The black circles indicate the forecast for the MSIE of 2007, 2008, and 2009 derived from SST of the OISST data in November and T850 of the NCEP-NCAR reanalysis data in October–November. Error bars indicate two standard deviation uncertainties.

Yasuda, 2010]. Figure 10b shows the annual mean surface dynamic topography at 100 m depth calculated from our data set. The northward flow west of the Kamchatska Peninsula in the Sea of Okhotsk, which is part of the Sverdrup cyclonic gyre [*Ohshima et al.*, 2004], can be recognized as well as the southwestward flow of the EKC. Inferred from the dynamic topography, the pattern around the Kamchatska Peninsula seen from Figure 10a would exist or be stronger in the absolute flow field. Thus, the ocean current field supports that the temperature anomaly in the EKC affects the MSIE by advective ocean heat flux.

4. Statistical MSIE Prediction Model

[25] As shown in section 3.2, it was found that the SST in the EKC is significantly correlated with the MSIE even if the contribution of the atmospheric conditions is excluded. Since the SST leads the MSIE by 2–3 months, use of the SST as well as T850 would permit the development of a more precise prediction scheme for the MSIE than that using only T850 data [*Sasaki et al.*, 2007]. Thus, we built a statistical prediction scheme for the MSIE based on the SST and T850 data by multiple linear regression as follows:

$$y(t) = -0.20x_1(t) - 0.05x_2(t) + 1.08, \quad (3)$$

where y represents the MSIE ($\times$ 10^6 km^2) in the Sea of Okhotsk, x_1 is the SST (°C) averaged in the EKC region in the preceding November–December, and x_2 is the T850 (°C) in the preceding October–November at 52.5°N, 135°E. When T850 and SST are normalized in scheme (3), the regression coefficients become −0.81 and −0.80, respectively, showing that the contribution of the two variables is almost the same in the prediction scheme. The correlation between the predicted and observed MSIE becomes 0.84 (71% of the total variance of the MSIE is explained by the two variables), which is 20% higher than the value of 0.71 (50% of the total variance) from the prediction using only the T850. Even if we use the SST in November instead of that in November–December in the scheme (3), the correlation between the predicted and observed MSIE is still 0.82. Figure 11 shows the time series of the predicted MSIE from the scheme (3) and observed MSIE, demonstrating the good correspondence between them. The high correlation at the stage of 2 to 3 months before the MSIE season and Figure 11 imply that the prediction scheme can be used operationally.

[26] Here, we have attempted the prediction of MSIEs for recent 3 years (2007, 2008, and 2009) based on the scheme (3). For the SST and T850, we used monthly mean OISST data [*Reynolds et al.*, 2002] and NCEP-NCAR reanalysis data, respectively. These monthly mean data are available by about the 10th of the next month. If we use the November SST and the October–November T850, we can predict MSIE at least 2.5 months in advance. In Figure 11, the recent MSIEs calculated from the HadISST (bars) and their predictions (circles) are plotted. It is found that the recent MSIEs could be predicted to some extent.

5. Summary and Discussion

[27] In this study, the relationship between the MSIE and ocean temperature is examined using various SST data sets and all available oceanographic data. It is found that the MSIE is significantly correlated with the ocean temperature around the EKC region in the preceding November–December. We examined the possibility that prevailing atmospheric variabilities affect both the SST and the MSIE. The relationship between them cannot be explained only by the atmospheric conditions in and around the Okhotsk Sea in autumn and winter as well as by the global-scale atmospheric modes. On the other hand, the ocean current data show that the EKC water is effectively transported to the Sea of Okhotsk in winter. These results suggest that the oceanic advection of the anomalous ocean temperature in the EKC influences the MSIE.

[28] We also demonstrate that the SST variation in the EKC can be useful for the prediction of the MSIE. 71% of the total variance of the MSIE is explained by a multiple regression model constructed as a function of SST in the EKC and the air temperature at 850 hPa over the upwind region of the Okhotsk Sea in late autumn, which is another determinant factor for the MSIE. The SST in the EKC and the upwind air temperature are related to the sea ice extent in the northeastern and center to southern parts of the Okhotsk

Sea, respectively. Since the prediction scheme using only the T850 explains 50% of the total variance [*Sasaki et al.*, 2007], the skill of our prediction scheme with both the SST and T850 is 20% higher than that using only the T850. Thus, the SST in the EKC significantly improves the prediction skill of the MSIE.

[29] Although our results suggest that the thermal condition in the EKC affects the MSIE through oceanic advection, there still remain the following questions. First, can the water around the EKC in November–December reach the northeastern part of the Okhotsk Sea by February–March? Second, can the thermal anomaly in the EKC water persist during winter?

[30] It has been reported that the EKC has surface velocity with average 20 to 40 $cm \cdot s^{-1}$ in December–February from satellite-tracked drifting buoy data [*Stabeno et al.*, 1994]. Since the distance between the area off the Kamchatska Peninsula and the northern part of the Kuril Straits is about 1,000 km, the ocean temperature anomaly in the EKC can be advected to the Sea of Okhotsk in a month or two. To explain a time lag of 2–3 months between the SST in the EKC and the MSIE, the EKC water in the northern part of the Kuril Strait must be transported to the northeastern part of the Okhotsk Sea in a month or two. This implies that the northward current speed in the eastern part of the Okhotsk Sea needs the order of 10 cm s^{-1}. Although there is no direct observation for the surface current in the eastern part of the Okhotsk Sea, the surface current data of the model simulation based on the eddy-resolving (1/12° grid) OGCM of the North Pacific developed at the Meteorological Research Institute [*Ishikawa and Ishizaki*, 2009] suggest that such a surface current exists along the East Kamchatska Peninsula within the Okhotsk Sea in winter.

[31] On the other hand, due to strong tidal mixing, extremely cold SST area occurs along the Kuril Islands in summer [*Nakamura and Awaji*, 2004]. Such a mixing may affect temperature anomalies even in winter. On the way to the northeastern part of the Okhotsk Sea, sea surface temperature is also affected by local atmospheric cooling. Thus, the quantitative estimation of the advected oceanic heat flux associated with the anomalous SST in the EKC should be examined in the future work after these uncertainties will be more clarified.

[32] Based on the historical sea ice extent data since 1970, it was shown that the sea ice extent variation in January–February is explained to some extent by the NAO [*Yamazaki*, 2000] and Aleutian low strength [e.g., *Tachibana et al.*, 1996], while the contributions of these large-scale atmospheric conditions are relatively weak on the MSIE variation, as presented in this study. *Kimura and Wakatsuchi* [1999] showed that the offshore component of the geostrophic wind over the Okhotsk Sea in winter is significantly correlated with the MSIE during the period from 1987 to 1996, while the correlation between the MSIE and the geostrophic wind is insignificant for longer period of the past 27 years (Table 1). Since the MSIE is relatively small in the period from 1987 to 1996, this difference can be interpreted as follows: the wintertime atmospheric condition affects on the MSIE only during the relatively small MSIE period. In brief, the extent that the sea ice finally reaches, where the northeastern region is a key area, is considered to be determined effectively by the ocean thermal condition rather than the wintertime atmospheric condition.

[33] **Acknowledgments.** Part of the hydrographic data in the Sea of Okhotsk were obtained in cooperation with the Far Eastern Regional Hydrometeorological Research Institute, Scripps Institute of Oceanography, and S. C. Riser of the University of Washington. Digital data of daily sea ice concentration in the Sea of Okhotsk from 1979 to 2006 were provided by N. Kimura. The surface current data of the model simulation based on an eddy-resolving OGCM of the North Pacific developed at the Meteorological Research Institute are provided by I. Ishikawa and T. Motoi. The altimeter products were produced by SSALTO/DUACS and distributed by AVISO with support from CNES. Hydrographical data were analyzed on the Pan-Okhotsk Information System of Hokkaido University. We wish to thank anonymous reviewers for their constructive comments. Some figures are produced with the GrADS package developed by B. Doty. This work was supported by Grant-in-Aid for Scientific Research (17310002 and 20221001).

References

Boyer, T. P., J. I. Antonov, H. E. Garcia, D. R. Johnson, R. A. Locarnini, A. V. Mishonov, M. T. Pitcher, O. K. Baranova, and I. V. Smolyar (2006), *World Ocean Database 2005, NOAA Atlas NESDIS*, vol. 60, edited by S. Levitus, 190 pp., U.S. Gov. Print. Off., Washington, D. C.

Cavalieri, D. J., and C. L. Parkinson (1987), On the relationship between atmospheric circulation and fluctuations in the sea ice extents of the Bering and Okhotsk seas, *J. Geophys. Res.*, *92*, 7141–7162.

Deser, C., J. E. Walsh, and M. S. Timlin (2000), Arctic sea ice variability in the context of recent atmospheric circulation trends, *J. Clim.*, *13*, 617–633.

Ducet, N., P. Y. Le Traon, and G. Reverdin (2000), Global high-resolution mapping of ocean circulation from TOPEX/Poseidon and ERS-1 and -2, *J. Geophys. Res.*, *105*, 19,477–19,498.

Honda, M., K. Yamazaki, H. Nakamura, and K. Takeuchi (1999), Dynamic and thermodynamic characteristics of atmospheric response to anomalous sea-ice extent in the Sea of Okhotsk, *J. Clim.*, *12*, 3347–3358.

Inoue, J., J. Ono, Y. Tachibana, M. Honda, K. Iwamoto, Y. Fujiyoshi, and K. Takeuchi (2003), Characteristics of heat transfer over the ice-covered Sea of Okhotsk during cold air outbreaks, *J. Meteorol. Soc. Jpn.*, *81*, 1057–1067.

Ishikawa, I., and H. Ishizaki (2009), Importance of eddy representation for modeling the intermediate salinity minimum in the North Pacific: Comparison between eddy-resolving and eddy-permitting models, *J. Oceanogr.*, *65*, 407–426.

Kanamitsu, M., W. Ebisuzaki, J. Woollen, S. K. Yang, J. J. Hnilo, M. Fiorino, and G. L. Potter (2002), NCEP-DOE AMIP-II reanalysis (R-2), *Bull. Am. Meteorol. Soc.*, *83*, 1631–1643.

Kaplan, D., and L. Glass (1995), *Understanding Nonlinear Dynamics*, 420 pp., Springer, New York.

Katsumata, K., and I. Yasuda (2010), Estimates of non-tidal exchange transport between the Sea of Okhotsk and the North Pacific, *J. Oceanogr.*, *66*, 489–504.

Kimura, N., and M. Wakatsuchi (1999), Processes controlling the advance and retreat of sea ice in the Sea of Okhotsk, *J. Geophys. Res.*, *104*, 11,137–11,150.

Levitus, S., and T. P. Boyer (1994), *World Ocean Atlas 1994*, vol. 4, *Temperature, NOAA Atlas NESDIS*, vol. 4, 129 pp., NOAA, Silver Spring, Md.

Nakamura, T., and T. Awaji (2004), Tidally induced diapycnal mixing in the Kuril Straits and its role in water transformation and transport: A three-dimensional nonhydrostatic model experiment, *J. Geophys. Res.*, *109*, C09S07, doi:10.1029/2003JC001850.

Ogi, M., and Y. Tachibana (2006), Influence of the annual Arctic Oscillation on the negative correlation between Okhotsk Sea ice and Amur River discharge, *Geophys. Res. Lett.*, *33*, L08709, doi:10.1029/2006GL025838.

Ohshima, K. I., D. Simizu, M. Itoh, G. Mizuta, Y. Fukamachi, S. C. Riser, and M. Wakatsuchi (2004), Sverdrup balance and the cyclonic gyre in the Sea of Okhotsk, *J. Phys. Oceanogr.*, *34*, 513–525.

Ohshima, K. I., S. Nihashi, E. Hashiya, and T. Watanabe (2006), Interannual variability of sea ice area in the Sea of Okhotsk: Importance of surface heat flux in fall, *J. Meteorol. Soc. Jpn.*, *84*, 907–919.

Ohshima, K. I., T. Nakanowatari, S. Riser, and M. Wakatsuchi (2010), Seasonal variation in the in- and outflow of the Okhotsk Sea with the North Pacific, *Deep Sea. Res., Part II*, *57*, 1247–1256.

Parkinson, C. L. (1990), The impact of the Siberian high and Aleutian low on the sea-ice cover of the Sea of Okhotsk, *Ann. Glaciol.*, *14*, 226–229.

Parkinson, C. L., and D. J. Cavalieri (2008), Arctic sea ice variability and trends, 1979–2006, *J. Geophys. Res.*, *113*, C07003, doi:10.1029/2007JC004558.

Rayner, N. A., D. E. Parker, E. B. Horton, C. K. Folland, L. V. Alexander, D. P. Rowell, E. C. Kent, and A. Kaplan (2003), Global analyses of sea surface temperature, sea ice, and night marine air temperature since the late nineteenth century, *J. Geophys. Res.*, *108*(D14), 4407, doi:10.1029/2002JD002670.

Reynolds, R. W., N. A. Rayner, T. M. Smith, D. C. Stokes, and W. Wang (2002), An improved in situ and satellite SST analysis for climate, *J. Clim.*, *15*, 1609–1625.

Reynolds, R. W., T. M. Smith, C. Liu, D. B. Chelton, K. S. Casey, and M. G. Schlax (2007), Daily high-resolution-blended analyses for sea surface temperature, *J. Clim.*, *20*, 5473–5496.

Sasaki, Y. N., Y. Katagiri, S. Minobe, and I. G. Rigor (2007), Autumn atmospheric preconditioning for interannual variability of wintertime sea-ice in the Okhotsk Sea, *J. Oceanogr.*, *63*, 255–265.

Stabeno, P. J., R. K. Reed, and J. E. Overland (1994), Lagrangian measurements in the Kamchatka Current and Oyashio, *J. Oceanogr.*, *50*, 653–662.

Tachibana, Y., M. Honda, and K. Takeuchi (1996), The abrupt decrease of the sea ice over the southern part of the Sea of Okhotsk in 1989 and its relation to the recent weakening of the Aleutian low, *J. Meteorol. Soc. Jpn.*, *74*, 579–584.

Trenberth, K. E., and J. W. Hurrell (1994), Decadal atmosphere-ocean variations in the Pacific, *Clim. Dyn.*, *9*, 303–319.

Worley, S. J., S. D. Woodruff, R. W. Reynolds, S. J. Lubker, and N. Lott (2005), ICOADS Release 2.1 data and products, *Int. J. Climatol.*, *25*, 823–842.

Yamazaki, K. (2000), Interaction between the wintertime atmospheric circulation and the variation in the sea ice extent of the Sea of Okhotsk (in Japanese with English abstract), *Seppyo*, *62*, 345–354.

S. Nagai, ITO-Ya Company, Tokyo, 104-0061, Japan.

T. Nakanowatari and K. I. Ohshima, Institute of Low Temperature Science, Hokkaido University, Kita-19, Nishi-8, Kita-ku, Sapporo, 060-0819, Japan. (nakano@lowtem.hokudai.ac.jp)